Nonlinear Dynamics and Systems Theory, **25** (5) (2025) 535–545

The Duffing Oscillator: Metamorphoses of 1 : 2 Resonance and Its Interaction with the Primary Resonance

J. Kyzioł and A. Okniński *

Politechnika Świętokrzyska, Al. 1000–lecia PP 7, 25-314 Kielce, Poland

Received: November 7, 2024; Revised: August 30, 2025

Abstract: We investigate the 1 : 2 resonance in the periodically forced asymmetric Duffing oscillator, it is created via the period-doubling of the primary 1 : 1 resonance or forming independently and coexisting with the primary resonance. We compute the steady-state asymptotic solution – the amplitude-frequency response function. Working in the framework of differential properties of implicit functions, we discover and describe complicated metamorphoses of the 1 : 2 resonance and its interaction with the primary resonance.

Keywords: *Duffing equation; resonances; singularities; metamorphoses.*

Mathematics Subject Classification (2020): 34C05, 34C25, 34E05, 37G35, 70K20, 70K30, 70K50.

1 Introduction and Motivation

A period-doubling cascade of bifurcations is a typical route to chaos in nonlinear dynamical systems. A generic example is the asymmetric Duffing oscillator governed by the non-dimensional equation

$$\ddot{y} + 2\zeta\dot{y} + \gamma y^3 = F_0 + F\cos(\Omega t)\,, \tag{1}$$

which has a single equilibrium and a one-well potential [1], where ζ, γ, F_0, F are parameters and Ω is the angular frequency of the periodic force.

Szemplińska-Stupnicka elucidated the period-doubling scenario in the dynamical system (1) in a series of far-reaching papers [2–4]; see also [1] for a review and further results.

* Corresponding author: mailto:fizao@tu.kielce.pl

The main idea introduced in [2] consists in perturbing the main steady-state (approximate) asymptotic solution of Eq.(1)

$$y_0(t) = A_0 + A_1 \cos(\Omega t + \theta) \tag{2}$$

as

$$y(t) = y_0(t) + B \cos\left(\tfrac{1}{2}\Omega t + \varphi\right), \tag{3}$$

substituting $y(t)$ into Eq.(1) and considering the condition $B \neq 0$. In papers [1–4], the authors found several conditions guaranteeing the formation and stability of solution (3) and used them to study the period-doubling phenomenon.

In our recent work, we studied the period-doubling scenario using the period-doubling condition determined in [1–4] as an implicit function. More precisely, using the formalism of differential properties of implicit functions [5,6], we derived analytic formulas for the birth of period-doubled solutions [7].

The motivation of this work stems from two observations: (i) In some cases, $1:2$ resonance, coexisting with $1:1$ resonance, is not created via the period doubling of $1:1$ resonance, and (ii) $1:2$ resonance depends on the parameters in a more complicated way than the primary resonance.

Thus, the present work aims to study the metamorphoses of the $1:2$ resonance coexisting with the primary $1:1$ resonance.

The paper is structured as follows. Section 2 describes the amplitude-frequency response, an implicit function, for the $1:2$ resonance for Eq.(1). In Section 3, we derive equations to compute singular points and vertical tangencies of the response function. Section 4 presents an example of the metamorphoses of $1:2$ resonance based on computed singular points. Section 5 provides an example of similar metamorphoses for a different dynamical system, suggesting a greater generality of our results. We summarize our results in the last section.

2 The $1:2$ Resonance: Steady-State Solution

Since the stable $1:2$ resonance can coexist with the stable primary $1:1$ resonance, we assume the following steady-state solution of Eq.(1):

$$y(t) = B_0 + B \cos\left(\tfrac{1}{2}\Omega t + \varphi\right), \tag{4}$$

which can be computed by proceeding as in [8,9]. More exactly, we get

$$\frac{3}{2}\gamma B_0 B^2 + \gamma B_0^3 + \frac{3}{2}\gamma B_0 C^2 - F_0 + \frac{3}{4}\gamma B^2 C \cos 2\varphi = 0, \tag{5a}$$

$$\zeta B\Omega - 3\gamma B_0 B C \sin 2\varphi = 0, \tag{5b}$$

$$\frac{1}{4}B\Omega^2 - \frac{3}{4}\gamma B^3 - 3\gamma B_0^2 B - \frac{3}{2}\gamma B C^2 - 3\gamma B_0 B C \cos 2\varphi = 0, \tag{5c}$$

where

$$C = \frac{4F}{3\gamma B^2 - 4\Omega^2}, \quad \left(3\gamma B^2 - 4\Omega^2 \neq 0\right). \tag{5d}$$

We note that in papers [1,2], a form describing a combination of $1:1$ and $1:2$ resonances was assumed (see Eq.(8.5.20) in [1] and Eq. (8a) in [2]), and thus, different equations for the asymptotic solution were obtained.

Assuming $B \neq 0$, we get from Eqs.(5b), (5c),

$$\begin{aligned} S_1\left(B_0, B, \Omega; \zeta, \gamma, F\right) &= \zeta^2\Omega^2 + \left(\tfrac{1}{4}\Omega^2 - \tfrac{3}{4}\gamma B^2 - 3\gamma B_0^2 - \tfrac{3}{2}\gamma C^2\right)^2 \\ &\quad -9\gamma^2 B_0^2 C^2 = 0. \end{aligned} \tag{6}$$

Moreover, equations (5a) and (5c) lead to

$$\begin{aligned} S_2\left(B_0, B, \Omega; \zeta, \gamma, F_0, F\right) &= -B^2\Omega^2 + 3B^4\gamma - 12B^2\gamma B_0^2 + 6B^2\gamma C \\ &\quad -16\gamma B_0^4 - 24\gamma B_0^2 C^2 + 16 B_0 F_0 = 0. \end{aligned} \tag{7}$$

Equation (7) is quadratic concerning B_0^2. Therefore, we solve this equation for B_0^2,

$$\begin{aligned} &B_0^2 = -\tfrac{1}{4}B^2 + \tfrac{1}{12\gamma}\Omega^2 \pm \frac{\sqrt{f\left(B, \Omega; \zeta, \gamma, F\right)}}{3\gamma\left(3\gamma B^2 - 4\Omega^2\right)^2},\ \left(\gamma > 0,\ 3\gamma B^2 - 4\Omega^2 \neq 0\right) \\ &f\left(B, \Omega; \zeta, \gamma, F\right) = -81\Omega^2\zeta^2\gamma^4 B^8 + 108\gamma^3\left(4\Omega^4\zeta^2 - 3F^2\gamma\right)B^6 \\ &-108\Omega^2\gamma^2\left(8\Omega^4\zeta^2 - 9F^2\gamma\right)B^4 + 96\gamma\Omega^4\left(8\Omega^4\zeta^2 - 9F^2\gamma\right)B^2 \\ &-256\zeta^2\Omega^{10} + 192F^2\gamma\Omega^6 - 576F^4\gamma^2. \end{aligned} \tag{8}$$

We substitute the following expression for B_0:

$$B_0\left(B, \Omega\right) = \sqrt{-\frac{1}{4}B^2 + \frac{1}{12\gamma}\Omega^2 + \frac{\sqrt{f\left(B, \Omega; \zeta, \gamma, F\right)}}{3\gamma\left(3\gamma B^2 - 4\Omega^2\right)^2}} \tag{9}$$

to Eq.(7) (it turns out that we have to choose the plus sign) to get a complicated but valuable implicit non-polynomial function $L\left(B, \Omega; \zeta, \gamma, F_0, F\right) = 0$,

$$L\left(B, \Omega; \zeta, \gamma, F_0, F\right) = S_2\left(B_0\left(B, \Omega\right), B, \Omega; \zeta, \gamma, F_0, F\right). \tag{10}$$

3 Vertical Tangencies and Singular Points

Equations for vertical tangencies read

$$L\left(B, \Omega; \zeta, \gamma, F_0, F\right) = 0, \tag{11a}$$

$$\frac{\partial L\left(B, \Omega; \zeta, \gamma, F_0, F\right)}{\partial B} = 0, \tag{11b}$$

while equations for singular points are

$$L\left(B, \Omega; \zeta, \gamma, F_0, F\right) = 0, \tag{12a}$$

$$\frac{\partial L\left(B, \Omega; \zeta, \gamma, F_0, F\right)}{\partial B} = 0, \tag{12b}$$

$$\frac{\partial L\left(B, \Omega; \zeta, \gamma, F_0, F\right)}{\partial \Omega} = 0. \tag{12c}$$

Equations (11), (12) can be solved numerically, yet simplify greatly for $B = 0$.

3.1 Vertical tangencies, $B = 0$

We check that

$$\left[\partial L\left(B, \Omega; \zeta, \gamma, F_0, F\right)/\partial B\right]_{B=0} = 0. \tag{13}$$

Therefore, we obtain a simplified equation for vertical tangencies

$$L\left(0,\Omega;\zeta,\gamma,F_0,F\right)=0. \tag{14}$$

We can solve equation (14) for Ω, getting

$$f_1\left(\Omega;\zeta,\gamma,F\right) = \Omega^{12}+16\zeta^2\Omega^{10}-12\gamma F^2\Omega^6+36\gamma^2F^4=0, \tag{15a}$$

$$f_2\left(\Omega;\zeta,\gamma,F_0,F\right) = \sum_{k=0}^{18}a_k\Omega^{2k}=0, \tag{15b}$$

and obtaining non-zero coefficients a_k as shown in Table 1 below.

For example, to find vertical tangencies, we can choose values of ζ, γ, F_0, and F, solve Eq.(15b), and accept all solutions with $\Omega>0$. Alternatively, we set ζ, γ, and F_0 and solve Eq.(15a), accepting solutions with $\Omega>0$.

k	a_k
18	1
17	$48\zeta^2$
16	$768\zeta^4$
15	$36\gamma F^2-3456\gamma F_0^2+4096\zeta^6$
14	$1152\zeta^2\gamma F^2+165\,888\zeta^2\gamma F_0^2$
13	$9216\gamma F^2\zeta^4$
12	$756\gamma^2F^4-248\,832\gamma^2F^2F_0^2+2985\,984\gamma^2F_0^4$
11	$24\,192\zeta^2\gamma^2F^4+1990\,656\gamma^2F^2F_0^2\zeta^2$
10	$193\,536\gamma^2F^4\zeta^4$
9	$3456\gamma^3F^6-2239\,488\gamma^3F^4F_0^2$
8	$165\,888\gamma^3F^6\zeta^2$
6	$-31\,104\gamma^4F^8+4478\,976\gamma^4F_0^2F^6$
5	$2488\,320\gamma^4F^8\zeta^2$
3	$-933\,120F^{10}\gamma^5$
0	$4665\,600F^{12}\gamma^6$

Table 1: Non-zero coefficients a_k of the polynomial (15b).

3.2 Singular points, $B=0$

Moreover, we can significantly simplify the equation for singular points (12) in the case $B=0$. We note that for $B=0$, Eq.(14) solves first two of equations (12), thus to find a solution of Eq.(12c), it suffices to demand that the equation (15b) has a double root (equation (15a) has no physical double roots). To this end, we request that the discriminant of the polynomial $f_2\left(\Omega\right)$ vanishes or solve the equivalent set of equations

$$f_2\left(\Omega;\zeta,\gamma,F_0,F\right) = 0, \tag{16a}$$

$$\frac{\partial f_2\left(\Omega;\zeta,\gamma,F_0,F\right)}{\partial\Omega} = 0. \tag{16b}$$

By solving Eqs.(16) for F_0, F, we obtain clear and simplified equations for singular points, making the computations easier,

$$p\left(Z\right)=d_{12}Z^{12}+d_{10}Z^{10}+d_8Z^8+d_6Z^6++d_4Z^4+d_2Z^2+d_0=0, \tag{17}$$

$$d_{12} = 466\,560\gamma^6,\ d_{10} = -233\,280\gamma^5\Omega^2,\ d_8 = 20\,736\gamma^4\Omega^2\left(2\Omega^2 + 11\zeta^2\right),$$
$$d_6 = -1728\gamma^3\Omega^4\left(2\Omega^2 + 41\zeta^2\right),\ d_4 = 54\gamma^2\Omega^4\left(3\Omega^4 + 112\zeta^2\Omega^2 + 448\zeta^4\right),$$
$$d_2 = -3\gamma\Omega^6\Omega^4 + 72\zeta^2\Omega^2 + 896\zeta^4,\ d_0 = 4\zeta^2\Omega^6\left(\Omega^4 + 20\zeta^2\Omega^2 + 64\zeta^4\right),$$

where $Z = \dfrac{F}{\Omega^2}$, and

$$q\left(T\right) = e_2T^2 + e_0 = 0, \tag{18}$$

$$e_2 = 1728\gamma\Omega^6 + 41\,472\gamma\zeta^2\Omega^4 + 1603\,584\gamma\zeta^4\Omega^2 + 22\,118\,400\gamma\zeta^6,$$
$$e_0 = -\Omega^{14} + \left(-534Z^2\gamma + 592\zeta^2\right)\Omega^{12} + \left(\begin{array}{l} 15\,768Z^4\gamma^2 - 31\,968Z^2\zeta^2\gamma \\ +20\,128\zeta^4 \end{array}\right)\Omega^{10}$$
$$+\left(-247\,968Z^6\gamma^3 + 627\,552Z^4\zeta^2\gamma^2 - 499\,008Z^2\zeta^4\gamma + 195\,072\zeta^6\right)\Omega^8$$
$$+\left(\begin{array}{l} 1736\,640Z^8\gamma^4 - 3805\,056Z^6\zeta^2\gamma^3 + 2596\,608Z^4\zeta^4\gamma^2 \\ -958\,464Z^2\zeta^6\gamma + 458\,752\zeta^8 \end{array}\right)\Omega^6$$
$$+\left(\begin{array}{l} -4199\,040Z^{10}\gamma^5 + 9642\,240Z^8\zeta^2\gamma^4 + 7617\,024Z^6\zeta^4\gamma^3 \\ -40\,255\,488Z^4\zeta^6\gamma^2 + 16\,465\,920Z^2\zeta^8\gamma \end{array}\right)\Omega^4$$
$$+\left(-19\,906\,560Z^{10}\zeta^2\gamma^5 - 76\,308\,480Z^8\zeta^4\gamma^4 + 23\,224\,320Z^6\zeta^6\gamma^3\right)\Omega^2$$
$$-99\,532\,800Z^{10}\zeta^4\gamma^5,$$

where $T = F_0\Omega$.

4 Numerical Verification

In this section, we shall compute singular points and vertical tangencies for the implicit function $L\left(B, \Omega; \zeta, \gamma, F_0, F\right) = 0$, Eq.(10), for chosen values of ζ, γ, and Ω. In the case $B = 0$, we use Eqs. (16) in the reduced forms (17) and (18) to compute singular points and apply Eqs.(15) to compute vertical tangencies. Then, in the case $B \neq 0$, we use Eqs.(12) and (11), respectively.

In what follows, we arbitrarily choose $\zeta = 0.09$, $\gamma = 0.3$, $\Omega = 1.5$.

4.1 Singular points and vertical tangencies, $B = 0$

Thus, we choose the singular point as $(B,\ \Omega) = (0,\ 1.5)$. We must compute the parameters F_0 and F, for which the selected point is singular.

Therefore, for $\zeta = 0.09$, $\gamma = 0.3$, $\Omega = 1.5$, and $B = 0$, we solve the equation $p\left(Z\right) = 0$ with $p\left(Z\right)$ defined in Eq.(17), obtaining four positive roots, $Z = 0.\,198\,445$, $0.\,509\,084$, $1.\,095\,980$, $1.\,259\,811$. We check, however, that only $Z = 1.\,095\,980$ leads to a solution of (12). Since $Z = F/\Omega^2$, we get, for $Z = 1.\,095\,980$, $F = 2.465\,955$. We now solve $q\left(T\right) = 0$ with $q\left(T\right)$ defined in Eq.(18), obtaining, for $Z = 1.\,095\,980$, one positive root $T = 0.112\,203$. Since $T = F_0\Omega$, we get $F_0 = 0.074\,802$.

Now, we check that for $\gamma = 0.3$, $F_0 = 0.074\,802$, $F = 2.465\,955$, equations (12), solved numerically, yield indeed $\zeta = 0.09$ and an isolated singular point $(B,\ \Omega) = (0,\ 1.5)$; see Fig.1 and Subsection 4.4 for description.

To find vertical tangencies, we set, for example, $\zeta = 0.082$ and use just computed parameter values $\gamma = 0.3$, $F_0 = 0.074\,802$, $F = 2.465\,955$. Solving equation (15b), we get $(B,\ \Omega) = (0,\ 1.\,474\,612)$, $(0,\ 1.\,527\,914)$ (all solutions of Eq.(15a) are complex); see red boxes in Fig.1.

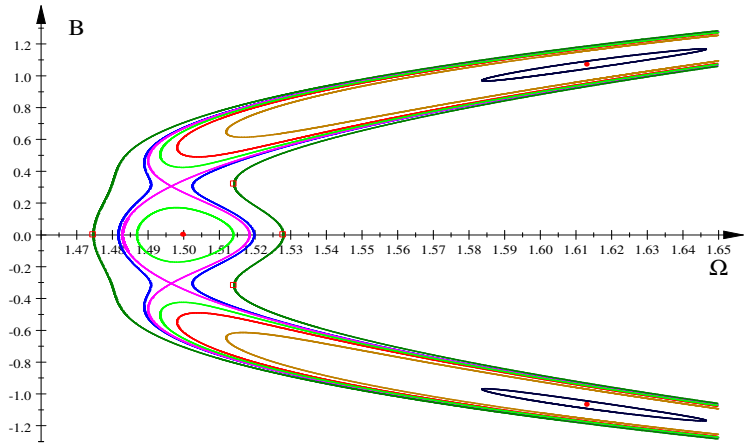

Figure 1: Sequential metamorphoses of amplitude-frequency implicit function $L(B, \Omega; \zeta, \gamma, F_0, F) = 0$, describing $1:2$ resonance.

4.2 Singular points and vertical tangencies, $B \neq 0$

We work with parameter values computed in the preceding subsection, i.e., $\gamma = 0.3$, $F_0 = 0.074\,802$, $F = 2.465\,955$. We have shown in the prior section that equations (12) have, for $\zeta = 0.09$, an isolated singular point $(B, \Omega) = (0, 1.5)$.

Moreover, equations (12) have other singular points for $\gamma = 0.3$, $F_0 = 0.074\,802$, $F = 2.465\,955$, and $B \neq 0$. Solving numerically Eqs.(12), we get (i) $\zeta = 0.086\,504$ and a pair of self-intersections $(B, \Omega) = (\pm 0.305\,755, 1.496\,498)$, (ii) a pair of isolated points, $\zeta = 0.108\,010$, $(B, \Omega) = (\pm 1.069\,257, 1.613\,277)$, see Fig.1 where we show all singular points.

We also compute vertical tangencies for $B \neq 0$. Solving equations (11a) and (11b) numerically for γ, F_0, F listed above and $\zeta = 0.082$, we get $(B, \Omega) = (\pm 0.318\,833, 1.514\,052)$; see red boxes in Fig.1.

4.3 Bifurcation diagrams

We have computed bifurcation diagrams solving Eq.(1) numerically – obtaining $y(t)$ as a function of Ω; for computational details, see Appendix A. Comparison with Fig.1 reveals which branches are stable. Colors in the bifurcation diagrams correspond to those in Fig.1, resonance $1:1$ is black.

We show, in Fig.2, the birth of $1:2$ resonance ($\zeta = 0.114\,69$, red; top figure), its growth ($\zeta = 0.114$, navy; top figure), and one period-doubling ($\zeta = 0.0977$, sienna; bottom figure).

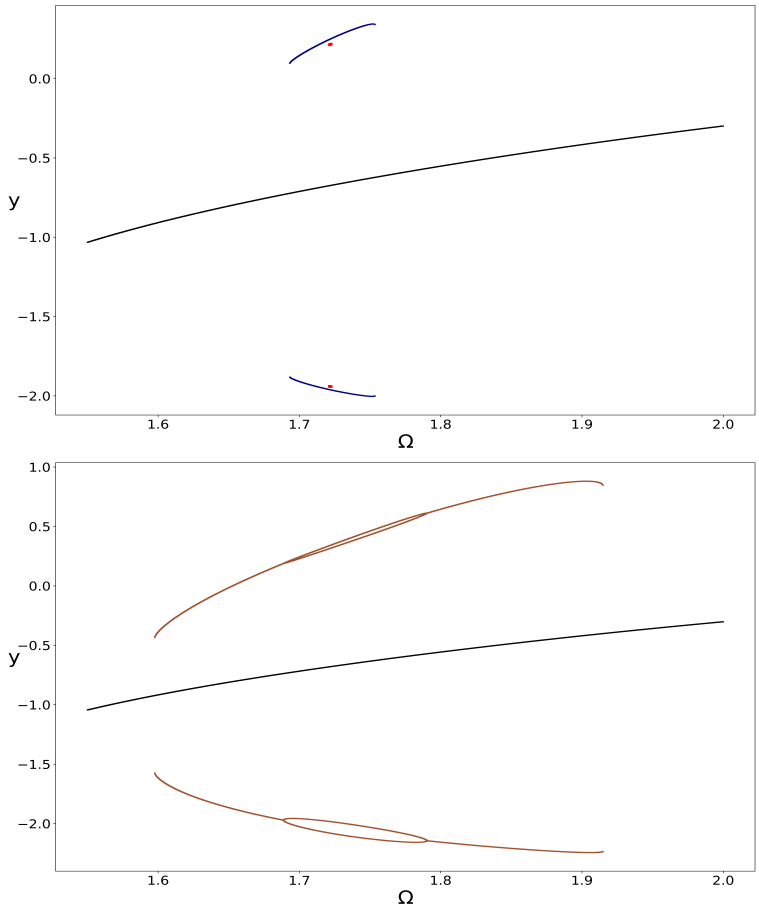

Figure 2: Bifurcation diagrams, $\zeta = 0.11469$ (two red boxes), $\zeta = 0.114$ (navy) – top, $\zeta = 0.0977$ (sienna) – bottom.

Figure 3 displays the first point of contact of $1:2$ resonance ($\zeta = 0.094185$, red circle; top figure) with $1:1$ resonance (black).

This singular point grows into an oval ($\zeta = 0.091$, green; bottom figure); a double period-doubling cascade forms and breaks.

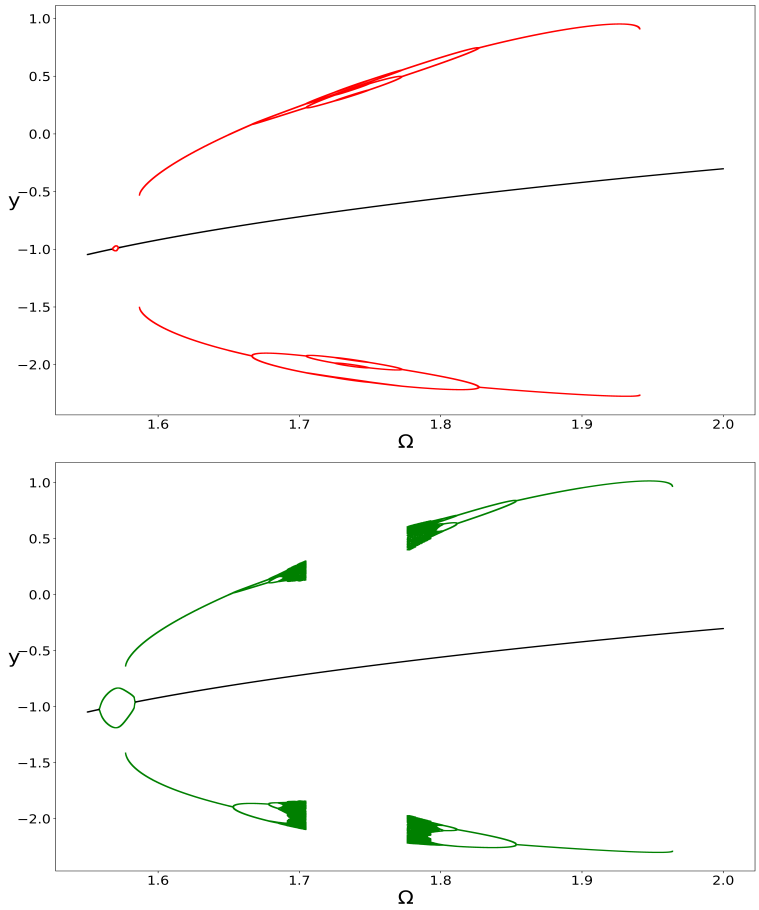

Figure 3: Bifurcation diagrams, $\zeta = 0.094\,185$ (top), $\zeta = 0.091$ (bottom).

Finally, in Fig.4, we display the formation of a double self-intersection ($\zeta = 0.090\,14$, magenta; top figure) and its subsequent breaking ($\zeta = 0.90$, blue; bottom figure).

We note that resonance $1:1$ and left resonance $1:2$ merge (top figure), then connected branches split in another way (bottom figure).

Section 4.4 describes in detail the complicated metamorphoses of $1:2$ resonance and its interaction with $1:1$ resonance.

4.4 Description of transmutations of $1:2$ resonance

We describe the metamorphoses of $1:2$ resonance for $\gamma = 0.3$, $F_0 = 0.074\,802$, $F = 2.465\,955$ and descending values of ζ. In what follows, ζ_n denotes the values of ζ computed by integrating the Duffing equation (1) numerically, while ζ_a means values of ζ computed from the analytical condition (12) for singular points. We have computed the function $L\,(B, \Omega; \zeta, \gamma, F_0, F)$, Eq.(10), from the asymptotic solutions (4) and (5).

In Fig.1, the transmutations of function $L\,(B, \Omega; \zeta, \gamma, F_0, F)$ are shown, and in bifurcation diagrams, Figs 2, 3 and 4, the metamorphoses of the solutions of the Duffing equation (1) are presented.

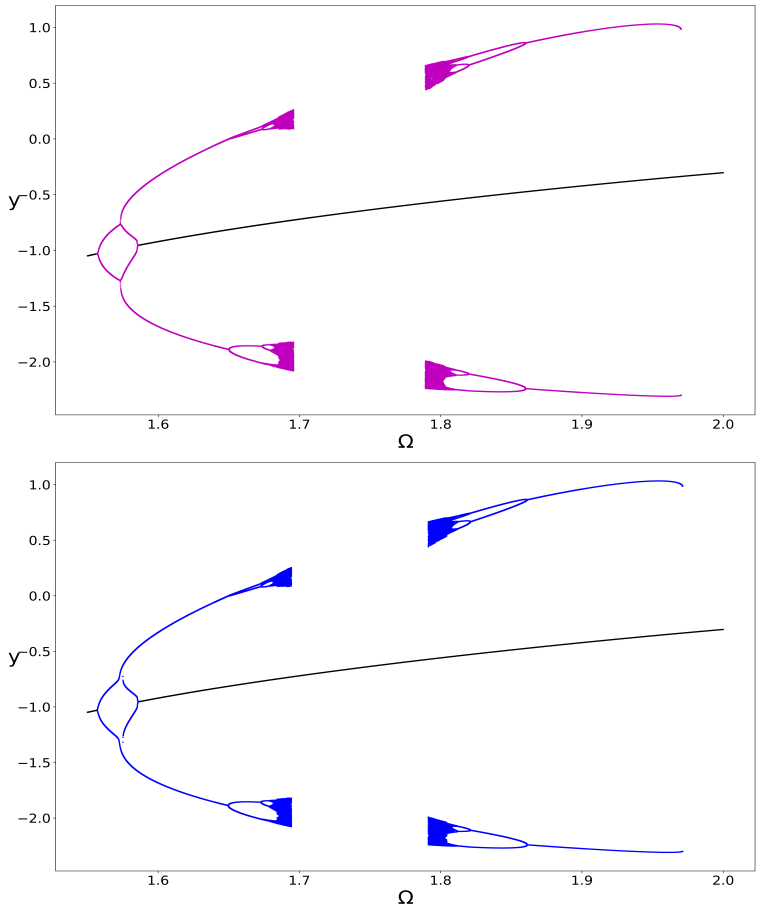

Figure 4: Bifurcation diagrams, $\zeta = 0.090\,14$ (top), $\zeta = 0.90$ (bottom).

Parameters in Fig.1 are $\gamma = 0.3$, $F_0 = 0.07480195$, $F = 2.\,465\,954$, and $\zeta_a = 0.108\,010$ (two red dots), $\zeta = 0.107\,2$ (navy), 0.095 (sienna), $\zeta_a = 0.09$ (red, a dot and two branches), $\zeta = 0.088$ (light green, an oval and two branches), $\zeta_a = 0.086\,504$ (magenta, two self-intersections), $\zeta = 0.086$ (blue), 0.082 (green).

We note good qualitative correspondence between predicted transmutations shown in Fig.1 and the metamorphoses of the solutions of the Duffing equation documented in Figs.2, 3, and 4.

We describe these changes as follows.

1. For $\zeta_n = 0.114\,69$, the $1:2$ resonance appears for the first time at $\Omega_n = 1.722$; see two red boxes (singular, two isolated points) in the top Fig.2. The corresponding analytical values are $\zeta_a = 0.108\,010$, $\Omega_a = 1.613$; see two red dots in Fig.1. Next, for descending values of ζ, the $1:2$ resonance grows and transforms rapidly.
   For $\zeta_n = 0.114$, $1:2$ resonance becomes larger; see navy lines in top Fig.2. Then, for $\zeta_n = 0.097\,7$, there is a first period-doubling of $1:2$ resonance; see two sienna branches in bottom Fig.2.

2. For $\zeta_n = 0.094185$ ($\zeta_a = 0.09$), a new isolated point of $1:2$ resonance (red) appears on $1:1$ resonance (black) at $\Omega_n = 1.57$ ($\Omega_a = 1.5$); see small red circle in top Fig.3 or red dot in Fig.1. The primary $1:1$ resonance is black.
   It is the first contact of these resonances. Note that the $1:2$ resonance has been subject to more period-doubling.

3. The singular, isolated point gives rise to an oval – a period-doubling of $1:1$ resonance; see the light green line in Fig.1 and the green oval in bottom Fig.3. The $1:1$ resonance is black.
   There is still no other contact between the primary $1:2$ resonance and the $1:1$ resonance.
   There are already two whole cascades of period-doublings of $1:2$ resonance that have been disrupted and moved away; we call them left and right; see green lines in Fig.3).

4. For $\zeta_n = 0.09014$ ($\zeta_a = 0.086504$), there are two self-intersections (two singular points) at $\Omega_n = 1.573$ ($\Omega_a = 1.496$) and resonance $1:1$ and left resonance $1:2$ merge; see magenta lines in Fig.1 and top Fig.4. The right $1:2$ resonance stays separated. The primary $1:1$ resonance is black.

5. For $\zeta < \zeta_n = 0.09014$ ($\zeta_a < 0.086504$), connected branches split in another way; see blue lines in Fig.1 and Fig.4. The primary $1:1$ resonance (black) absorbs the left $1:2$ resonance with the whole cascade of period-doubling; there is also another branch of $1:1$ resonance, with one period-doubling. The right $1:2$ resonance stays unchanged.

Summing up, the separate $1:2$ resonance, after the first contact with $1:1$ resonance, splits into two parts, left and right, then the left resonance $1:2$ merges with the primary $1:1$ resonance and splits in another way.

5 Summary and Most Important Findings

Based on the amplitude-frequency steady-state implicit equation (10) computed for Eq.(1), we studied the metamorphoses of the resonance $1:2$ and its interaction with the primary resonance $1:1$.

Working within the formalism of the differential properties of implicit functions, we derived formulas to compute singular points of the amplitude-frequency function $L(B, \Omega; \zeta, \gamma, F_0, F)$ defined in (10), see Section 3. In Section 4, we have computed singular points for arbitrary parameters $\zeta = 0.09$, $\gamma = 0.3$, $\Omega = 1.5$.

It should be stressed that the dynamics of the initial equation (1) change in the neighborhood (in the parameter space) of singular points.

We also computed bifurcation diagrams by solving Eq.(1) numerically, see Figs.2, 3, and 4, and obtained good agreement with the amplitude-frequency profiles of Fig.1.

The most significant achievements of this work are:

1. The semi-analytic and numerical procedures to compute singular points of the amplitude-frequency implicit function (10) that indicate the birth of $1:2$ resonance, correspond to the first contact of resonances $1:2$ and $1:1$, and merging of $1:2$ and $1:1$ resonances.

2. Discovery and detailed description of complicated transmutations of 1 : 2 resonance that resulted in the first contact with the primary 1 : 1 resonance, disruption of the 1 : 2 resonance into two parts, left and right, merging of the left 1 : 2 resonance with the primary 1 : 1 resonance, and breaking again; the right 1 : 2 resonance effectively not evolving.

A Computational details

Nonlinear equations were solved numerically using the computational engine Maple 4.0 from Scientific WorkPlace 4.0. Figure 1 was plotted with the computational engine MuPAD 4.0 from Scientific WorkPlace 5.5. Bifurcation diagrams in Figs.2, 3, and 4 were computed by integrating numerically Eq.(1) running DYNAMICS [11], as well as our programs written in Pascal and Python [12].

References

[1] I. Kovacic and M.J. Brennan. Forced harmonic vibration of an asymmetric Duffing oscillator. In: *The Duffing Equation: Nonlinear Oscillators and Their Behavior*. (Eds.: I. Kovacic, M.J. Brennan). John Wiley & Sons, Hoboken, New Jersey 2011; pp. 277–322.

[2] W. Szemplińska-Stupnicka and J. Bajkowski. The 1/2 subharmonic resonance and its transition to chaotic motion in a non-linear oscillator. *Int. J. Nonlinear Mech.* **21** (1986) 401–419.

[3] W. Szemplińska-Stupnicka. Secondary resonances and approximate models of routes to chaotic motion in non-linear oscillators. *J. Sound and Vibration* **113** (1987) 155–172.

[4] W. Szemplińska-Stupnicka. Bifurcations of harmonic solution leading to chaotic motion in the softening type Duffing's oscillator. *Int. J. Nonlinear Mech.* **23** (1988) 257–277.

[5] G.M. Fikhtengol'ts. (I.N Sneddon, Ed.) *The fundamentals of mathematical analysis*, Vol. 2, Elsevier, 2014 (Chapter 19), translated from Russian, Moscow, 1969.

[6] J. Kyzioland A. Okniński. The Twin-Well Duffing Equation: Escape Phenomena, Bistability, Jumps, and Other Bifurcations. *Nonlinear Dynamics and Systems Theory* **24** (2024) 181–192.

[7] J. Kyzioland A. Okniński. Asymmetric Duffing oscillator: the birth and build-up of period doubling cascade. *J. Theor. Appl. Mechanics* **62** (2024) 713–719.

[8] K.L. Janicki and W. Szemplińska-Stupnicka. Subharmonic Resonances and Criteria for Escape and Chaos in a Driven Oscillator. *Journal of Sound and Vibration* **180** (1995) 253–269.

[9] K.L. Janicki. PhD Thesis (in Polish), Institute of Fundamental Technologicall Research PAS, 16/1994, `https://rcin.org.pl/dlibra/doccontent?id=686`.

[10] W. Szemplińska-Stupnicka. *Chaos, Bifurcations and Fractals Around Us: A Brief Introduction*. Vol. 47. World Scientific, 2003.

[11] Nusse, Helena E. and James A. Yorke. *Dynamics: numerical explorations: accompanying computer program dynamics*. Vol. 101. Springer, 2012.

[12] Fernando Pérez and Brian E. Granger. IPython: A System for Interactive Scientific Computing. *Computing in Science and Engineering* **9** (3) (2007) 21–29. doi:10.1109/MCSE.2007.53. URL: https://ipython.org.